Packet Size Optimization for Lifetime Maximization in Underwater Acoustic Sensor Networks

Huseyin Ugur Yildiz, *Member, IEEE*, Vehbi Cagri Gungor, and Bulent Tavli, *Senior Member, IEEE*

***Abstract*—Recently, underwater acoustic sensor networks (UASNs) have been proposed to explore underwater environments for scientific, commercial, and military purposes. However, long propagation delays, high transmission losses, packet drops, and limited bandwidth in underwater propagation environments make realization of reliable and energy-efficient communication a challenging task for UASNs. To prolong the lifetime of battery-limited UASNs, two critical factors (*i.e.*, packet size and transmission power) play vital roles. At one hand, larger packets are vulnerable to packet errors, while smaller packets are more resilient to such errors. In general, using smaller packets to avoid bit errors might be a good option. However, when small packets are used, more frames should be transmitted due to the packet fragmentation, and hence, network overhead and energy consumption increases. On the other hand, increasing transmission power reduces frame errors, but this would result in unnecessary energy consumption in the network. To this end, the packet size and transmission power should be jointly considered to improve the network lifetime. In this study, an optimization framework via an integer linear programming (ILP) has been proposed to maximize the network lifetime by joint optimization of the transmission power and packet size. In addition, a realistic link-layer energy consumption model is designed by employing the physical layer characteristics of UASNs. Extensive numerical analysis through the optimization model has been also performed to investigate the tradeoffs caused by the transmission power and packet size quantitatively.**

***Index Terms*—Integer linear programming (ILP), network lifetime, optimum packet size (OPS), transmission power control (TPC), underwater acoustic sensor networks (UASNs).**

Manuscript received August 19, 2017; revised January 22, 2018 and April 8, 2018; accepted May 18, 2018. Date of publication May 29, 2018; date of current version February 1, 2019. The work of V. C. Gungor was supported by The Scientific and Technological Research Council of Turkey (TUBITAK) 1001 Project (project no. 114E248). Paper no. TII-17-1855. *(Corresponding author: Huseyin Ugur Yildiz.)*

H. U. Yildiz is with the TED University, 06420, Ankara, Turkey (e-mail: hugur.yildiz@tedu.edu.tr).

V. C. Gungor is with the Abdullah Gul University, 38039, Kayseri, Turkey (e-mail: cagri.gungor@agu.edu.tr).

B. Tavli is with the TOBB University of Economics and Technology, 06560, Ankara, Turkey (e-mail: btavli@etu.edu.tr).

Color versions of one or more of the figures in this paper are available online at http://ieeexplore.ieee.org.

Digital Object Identifier 10.1109/TII.2018.2841830

I. Introduction

UNDERWATER acoustic sensor networks (UASNs) have drawn a great attraction by researches working on military and commercial aquatic applications. Some use cases of UASNs include oceanic data collection, pollution monitoring, long-term underwater exploration, tactical surveillance, *etc.* [1], [2]. Typical UASNs are formed with numerous sensor nodes that are arbitrarily distributed within a region and a base station (*i.e.*, sink node). Underwater sensor nodes gather data from the underwater habitat and transfer the captured data to the base station generally by using multihop communication schemes [3]. Since sensor nodes have scarce battery energy, recharging (or replacing) the batteries of sensor nodes is infeasible [4], [5]. Hence, the optimal utilization of energy consumption becomes an important research challenge in UASNs to attain energy efficiency [6], which yields a prolonged lifetime.

The characteristics of the underwater channel are severe when compared to terrestrial wireless channels. Some notorious features of underwater channels include high path loss (attenuation), frequent packet drops, multipath fading, dispersion of frequency, limited bandwidth (usually a few kilohertz), and long propagation delay caused by the speed of sound in water when considering large-scale UASNs [7]. There are several approaches to combat against the crucial nature of the underwater environment to maximize the network lifetime. Two possible solutions are packet size optimization (PSO) as well as transmission power control (TPC) according to the channel conditions.

The PSO has proven to have a great impact on the performance of UASNs [8]. Usage of larger frames is an acceptable option as long as the acoustic link quality is sufficient [9]. On the other hand, when channel conditions become harsh, which is a frequent occurrence in underwater channels [1], usage of smaller frames are favorable to reduce the frame error rates [10]. However, the price paid for this case is the extra data traffic injected through the network that leads to an overhead of energy dissipation [11]. Although reducing individual frame error rates is critical, data exchange may be performed through a handshaking mechanism [12], [13]. A possible method to perform handshaking is to notify the sender as long as the transmitted data packet is successfully received by using a small-sized acknowledgement (ACK) packet [14]. In such a case, minimizing the handshaking failure becomes more important than minimizing the individual frame errors.

The other important technique to elongate the network lifetime is to utilize TPC schemes [15], [16]. Larger packets that are susceptible to errors require less energy for communications, while smaller packets that are resilient to errors need more energy (due to the overhead data generated by fragmentation). Increasing the transmission power helps to minimize the handshaking errors but this method degrades the network energy efficiency. Adjusting transmission powers, according to the requirements of an UASN application, can be either applied at a network level (*i.e.*, usage of a global transmission power at all links) or at a link level (*i.e.*, carefully adjusting the transmission power at each link by considering the conditions of the link) [14]. Hence, determining the optimum transmission power with the packet size rises a tradeoff that should be carefully addressed for prolonging the lifetime of UASNs.

To address these challenges, we propose a novel optimization model based on the integer linear programming (ILP) to jointly explore the effects of the PSO and TPC on the network lifetime. In summary, our contributions can be listed as follows.

1) We develop a realistic link-layer handshake scheme [12], [17]–[19], which uses foundations of the well-studied physical-layer models for underwater communications [20], [21].
2) The proposed link-layer model adopts the power consumption characteristics of widely used six different commercial and experimental underwater modems (*i.e.*, EvoLogics S2CR 18/34 WiSE, WHOI Micromodem, Teledyne Benthos ATM9XX, LinkQuest UWM4000, Aquatech AQUAModem 1000, and DSPComm AquaComm Marlin [22]).
3) We built a novel optimization framework via the ILP that employs the principles of the proposed link-layer model aiming to determine the maximum lifetime of an UASN by jointly considering the PSO and TPC.
4) We investigate the impact of network-level and node-level TPC strategies on the determination of the optimum packet size (OPS) by using the novel ILP framework through the numerical evaluations.
5) We also determine the OPSs for several commercial and experimental underwater modems when considering different networking conditions.

The structure of this paper is provided as follows. Section II overviews the literature on the PSO in UASNs. In Section III, constructed physical, link-layer, and optimization models are introduced along with the proposed TPC approaches. Results of the numerical analysis are provided in Section IV. Finally, Section V provides outcomes of this paper.

II. Related Work

The last two decades have seen a growing trend toward the PSO in sensor networks. Some practical use cases of the PSO include terrestrial wireless sensor networks (WSNs) [23], [24], cognitive radio sensor networks [25], wireless body area sensor networks [26], terrestrial-sensor-network-based smart grid applications [27], and underground sensor networks [10]. Recently, we observe a growing body of the literature on the PSO in UASNs [3], [8]–[11], [18], [19], [28]–[33]. We present an overview of the literature on the PSO in UASNs as follows.

Stojanovic [8] uses the PSO to maximize the throughput efficiency at the link layer. However, this paper ignores the overhead caused by retransmissions or forward error correction (FEC) schemes. Xie and Cui [18] compare the random access and handshaking-based methods on the determination of the OPS. In [28], two distributed algorithms are proposed to maximize the energy efficiency and determine the OPS for data gathering applications in UASNs. The impact of the PSO on throughput for the MACA-U protocol (*i.e.*, underwater adaptation of the MACA protocol [17]) is elaborated in [19]. A cross-layer examination of the PSO is performed for terrestrial, underwater, and underground sensor networks in [10] by incorporating the FEC methods. Basagni *et. al.* [29] provided a comprehensive analysis to quantify the effects of the PSO on throughput, latency, and energy-per-bit consumption for different link-layer protocols. They also study the benefits of the PSO and usage of packet fragmentation in harsh environments in [30]. Besides, the authors incorporate the effects of interference and varying bit error rates in [3]. PSO and energy efficiency issues in conjunction with the FEC for shallow water acoustic channels are investigated in [31]. The relationship between the OPS, throughput, and packet errors by considering a two-hop ACK model is studied in [9]. Ahmad *et al.* [11] determined the OPS by considering the environmental factors such as temperature, pressure, salinity, *etc.* In [32], the impact of the PSO on the throughput of a link that is affected by mobility is investigated. In [33], authors propose an optimization model for energy efficiency that can satisfy both a given signal-to-noise ratio (SNR) at the physical layer as well as throughput at the link layer.

As a summary, the key performance metrics for the PSO in UASNs can be categorized as: throughput [3], [8], [10], [11], [18], [19], [29], [30], [32], [33], latency [3], [9], [10], [29], [30], energy efficiency [3], [10], [28]–[31], and packet error rate [3], [9], [10], [28]–[31].

Recent advancement of the sensor node hardware technology enables intelligent TPC mechanisms to be used for reducing the overall energy consumption in the network. One way of using the TPC is to devise a sleep/awake scheduling [7]. The other way is to adjust the transmission power according to the channel conditions. Considering the second case, adjustment of the transmission power can be applied at network level or at link level [14] as stated in the introduction section. Although consolidation of PSO and TPC are efficient ways to maximize the network lifetime, researchers should also put a special emphasis to ensure collision-free data exchanges to satisfy a predetermined quality of service in UASNs. Two promising methods to fight against collisions are the random access [34] and handshaking [12], [13]. In random access, the transmitter sends packets without any coordination, hence, packet avoidance occurs in a probabilistic manner [18]. On the other, handshaking-based protocols use small packets [*i.e.*, request-to-send (RTS) and clear-to-send (CTS)] before the data exchange starts to avoid collisions [12], [19]. Although the high propagation delay degrades the performance of handshaking in UASNs, this approach still can be used by utilizing an idle/wake (or a sleep/wake) mechanism for

low-duty-cycle applications [34] such as the network lifetime maximization problem as explored in this study. Moreover, it is shown that handshaking can perform better results in many UASN applications [18].

The closest study to ours is [27] where the impact of PSO and TPC on terrestrial WSNs deployed in smart grid environments are investigated through an optimization model. Indeed, an optimization model in this paper is inspired by the model in [27]. However, there are many significant differences between [27] and this study. First, [27] investigates terrestrial WSN-based smart grids, whereas this study is on UASNs. Second, the channel model in [27] is a log-normal shadowing-based wireless channel model where the shadowing component is modeled as a Gaussian random variable and the mean and variance of this random variable are derived experimentally, however, in this study, we adopt both an empirical model (*i.e.*, Urick's model) and an accurate ray tracing model (*i.e.*, BELLHOP model) to correctly model the complex nature of the underwater channel. Third, in [27], only a specific platform (*i.e.*, Tmote Sky) is modeled, yet, in this paper, we consider a total of six different commercial and research underwater modems (*i.e.*, EvoLogics S2CR 18/34 WiSE, WHOI Micromodem, Teledyne Benthos ATM9XX, LinkQuest UWM4000, Aquatech AQUAModem 1000, and DSPComm AquaComm Marlin).

Although PSO and TPC issues are studied extensively in terrestrial sensor networks, our work differs from these studies such that we propose a realistic link layer model that incorporates characteristics of underwater propagation, communication and power control techniques, and power consumption characteristics of different underwater modem platforms. In addition, there have been no studies in the literature on joint optimization of the transmission power and packet size to prolong UASN lifetime by using a realistic link-layer model.

III. System Model

In this section, we introduce the abstraction for the energy dissipation in the network, which is built onto a realistic physical model for UASNs; then we present our optimization framework that aims to maximize the network lifetime. In this section, we use power consumption characteristics of the EvoLogics S2CR 18/34 WiSE underwater modem [35], which operates in 18–34-kHz frequency band with a central operating frequency as $f = 26$ kHz. The reported electrical transmission powers for EvoLogics S2CR 18/34 WiSE are in the interval 2.8–35 W. For the sake of simplicity, we define set $\mathcal{L} = \{5, 10, 15, \ldots, 35\}$ to represent discrete transmission power levels used throughout this paper. In the analysis section (*i.e.*, Section IV), we also consider the energy dissipation characteristics of several other underwater modems available on the market and academia.

A. Physical Layer Model

We use the principles of the underwater acoustic path loss model (*i.e.*, Urick's model) presented in [21]. The path loss (attenuation) of the acoustic link-(i, j) (*i.e.*, $A_{ij}(f)$) in terms of decibel is given by

$$A_{ij}(f)[\text{dB}] = 10\kappa \log_{10}(1000 \times d_{ij}) + d_{ij}a(f)[\text{dB/km}] \quad (1)$$

where f is the central operating frequency (*i.e.*, $f = 26$ kHz for the S2CR 18/34 WiSE modem [35]), $\kappa = 2$ is the spreading factor accounted for the deep water spherical loss, d_{ij} is the distance of link-(i, j) in km, and $a(f)$ is the absorption coefficient (in dB/km) that is obtained by using the following Thorp's empirical formula [21]

$$a(f)[\text{dB/km}] = \frac{0.11f^2}{1+f^2} + \frac{44f^2}{4100+f^2} + 2.75 \cdot 10^{-4} f^2 + 0.003. \quad (2)$$

The ambient noise consists of turbulence $N_{\text{t}}(f)$, shipping $N_{\text{s}}(f)$, wind-driven waves $N_{\text{w}}(f)$, and thermal noise $N_{\text{th}}(f)$. These individual noise components can be calculated (in decibel re 1μ Pa per Hz) as follows [21]:

$$\begin{aligned} 10\log_{10} N_{\text{t}}(f) &= 17 - 30\log_{10} f \\ 10\log_{10} N_{\text{s}}(f) &= 40 + 20\,(s - 0.5) + 26\log_{10} f \\ &\quad - 60\log_{10}(f + 0.03) \\ 10\log_{10} N_{\text{w}}(f) &= 50 + 7.5\sqrt{w} + 20\log_{10} f \\ &\quad - 40\log_{10}(f + 0.4) \\ 10\log_{10} N_{\text{th}}(f) &= -15 + 20\log_{10} f. \end{aligned} \quad (3)$$

Hence, we can express the total noise power density in linear scale as $N(f) = N_{\text{t}}(f) + N_{\text{s}}(f) + N_{\text{w}}(f) + N_{\text{th}}(f)$, where $s = 0.5$ denotes a medium shipping activity factor and $w = 5$ is the wind speed in m/s.

By using the passive sonar equation [36], the SNR at node-j due to the transmission of node-i with power level-l (*i.e.*, $l \in \mathcal{L}$) is expressed as

$$\text{SNR}_{ij}(l, f)\,[\text{dB}] = P_{tx}^{ac}(l) - N(f)[\text{dB}] - A_{ij}(f)\,[\text{dB}] \quad (4)$$

where $P_{tx}^{ac}(l)$ is the transmit sound source level at power level-l (in dB re 1μ Pa). The electrical transmit power level-l in terms of watts, $P_{tx}^{\text{el}}(l)$, can converted to dB re 1μ Pa as [36]

$$10\log_{10} P_{tx}^{\text{el}}(l) = 10\log_{10} P_{tx}^{ac}(l) - 170.8 - 10\log_{10}\xi \quad (5)$$

where 170.8 dB accounts for the conversion from dB re 1μ Pa to Watts, and $\xi = 0.8$ is the efficiency of the transducer. We assume the binary phase shift keying (BPSK) as the modulation scheme where the probability of a successful M-byte frame reception at node-j that is transmitted from node-i by using the power level-l, is given as [37]

$$\rho_{ij}^{s}(l, f, M) = \left(1 - \frac{1}{2}\,\text{erfc}\sqrt{\text{SNR}_{ij}(l, f)\frac{B_N}{R}}\right)^{8\times M} \quad (6)$$

where $B_N = 1$ kHz is the noise bandwidth, $R = 13.9$ kb/s is the data rate of the S2CR 18/34 WiSE modem [35], and $\text{SNR}_{ij}(l, f)$ is in linear scale. Similarly, the packet error rate is calculated as $\rho_{ij}^{f}(l, f, M) = 1 - \rho_{ij}^{s}(l, f, M)$. Since we consider a fixed central frequency of operation, we omit the f notation throughout this paper.

Urick's model is a rough approximation for the path loss analysis, hence, practical applications based on this model may provide misleading results. In order to rigorously assess the complex physical layer conditions of an UASN, more accurate tools that can perform ray tracing should be used. One of the most popular ray tracing tools used in the UASN literature is called BELLHOP model that is designed to perform acoustic ray tracing for a given speed of the sound profile and absorbing boundary conditions [20]. The BELLHOP model produces ray coordinates, acoustic pressure, or transmission loss values as outputs [38]. Many of today's popular simulators such as SUNSET [39] and DESERT [40] have adopted both Urick and BELLHOP models in their libraries. The BELLHOP model has proven to be an accurate physical model tool for underwater communications operating at frequencies that are greater than 1 kHz [41], [42]. In the analysis section, results will be presented for both Urick and BELLHOP models. For the BELLHOP model, we adopt the parameters given in [41] such that we utilize an isospeed sound velocity profile (*i.e.*, $c = 1500$ m/s) and bottom sound speed is taken as $c_b = 1800$ m/s. We also assume that sea surface and floor are flat and densities of the seawater and bottom are taken as $\rho_s = 1024$ and $\rho_b = 1843$ kg/m^3, respectively.

B. Link-Layer Model

In this section, we describe our link-layer model that uses a slotted (rounded) communication scheme where each round is defined as 150 s. We define s_i to represent the number of data frames generated at each round. In this paper, we consider an underwater surveillance scenario where each node is equipped with an onboard camera that captures an image of 512× 512 pixels of image with 8 bits per pixel at each round. The raw image is assumed to be compressed by using JPEG-2000 with 0.01 compression rate that yields 2603 bytes of processed image data [43]. For the sake of simplicity, we assume that $L_D = 3000$ bytes of the image data are acquired by the sensor nodes, which are indented to be transferred to the base station at each round. We denote the payload size with L_{PL}, which can take one of the following: 3000, 1500, 750, 600, 500, 375, 300, 250, 200, 150, 100, 75, 50, and 30 bytes. Hence, if the payload size is adjusted as 3000 bytes, the sender node will transmit a single data frame (*i.e.*, $s_i = L_D/L_{\text{PL}} = 1$). However, if 30 bytes of the payload trunk is used, then the sender node transmits 100 data frames (*i.e.*, $s_i = 100$). This idea is valid for other payload sizes. The data frame has an additional 20-byte of header information ($L_H = 20$ bytes). Thus, the data frame size is calculated by $L_P = L_{\text{PL}} + L_H$ bytes. $L_A = 20$ bytes denotes the length of an ACK packet.

We define the active slot time of link-(i, j) as $t^s_{ij} = t(L_P) + t(L_A) + t^p_{ij} + t_g$. In this equation, $t(L_P)$ and $t(L_A)$ are times to transmit a data and an ACK frame. $t^p_{ij} = 2 \times \frac{d_{ij}}{c}$ is the round-trip propagation delay of link-(i, j). t_g is defined as the guard time duration, which is used to avoid collision during the transmission [44] and taken as twice the maximum propagation delay (*i.e.*, $2 \times \max_{(i,j)}(t^p_{ij})$) [34]. Time slots are cushioned by guard times from both ends to prevent synchronization errors.

While achieving a handshake with success, three possible cases may occur, which are enumerated as follows.

1) *Successful handshake:* Data and ACK frames are error free received at the intended nodes.
2) *Unsuccessful handshake—Case I:* Data frame can be received with no errors in the forward acoustic link, but the ACK frame may be dropped in the reverse acoustic channel.
3) *Unsuccessful handshake—Case II:* Data frame may be dropped in the forward acoustic link so that no ACK frames are transmitted in the reverse acoustic channel.

For unsuccessful handshake cases, a retransmission should be initiated to guarantee a successful data and ACK exchange.

Considering the basic handshaking mechanism stated previously, if a sender node-i transmits a data frame with the power level-l and receives an ACK packet, which is transmitted by the receiver node-j upon receiving the data packet with the power level-k, the probability of the successful handshake can be calculated as

$$\rho^s_{\text{HS},ij}(l,k) = \rho^s_{ij}(l, L_P) \times \rho^s_{ji}(k, L_A). \tag{7}$$

On the contrary, handshake error probability is $\rho^f_{\text{HS},ij}(l,k) = 1 - \rho^s_{\text{HS},ij}(l,k)$. If we consider a stop-and-wait automatic repeat request scheme for retransmissions [17], we need to transmit each data packet $\lambda^{lk}_{ij} = 1/\rho^s_{\text{HS},ij}(l,k)$ times on the average.

1) Energy Consumption of the Transmitting Node: If the handshake is successful as stated in case 1, the transmitter side consumes $P^{\text{el}}_{tx}(l) \times t(L_P)$ J for data transmission by using power level-l and $P_{rx} \times t(L_A)$ J for the ACK frame reception, where $P_{rx} = 1.3$ W is the reception power [35]. In the remaining slot time (*i.e.*, $\{t^s_{ij} - t(L_P) - t(L_A)\}$), the transmitter side would be in standby mode where $P_{\text{std}} \times \{t^s_{ij} - t(L_P) - t(L_A)\}$ J of energy is dissipated. Note that, $P_{\text{std}} = 2.5$ mW is the power expenditure for the standby mode [35]. Hence, the total energy dissipation for this case is

$$E^s_{tx,ij}(l,k) = \left[P_{\text{std}}\{t^s_{ij} - t(L_P) - t(L_A)\} + P^{\text{el}}_{tx}(l)t(L_P) + P_{rx}t(L_A)\right] \times \frac{\rho^s_{ij}(l, L_P)\rho^s_{ji}(k, L_A)}{\rho^s_{\text{HS},ij}(l,k)}. \tag{8}$$

On the other hand, if the handshake is unsuccessful as stated in case 2, the transmitter side dissipates $P^{\text{el}}_{tx}(l) \times t(L_P)$ J for data transmission. Since the ACK frame is dropped due to the channel conditions, the transmitter side does not dissipate the energy for ACK reception. Instead, the transmitter will be in the standby mode in the rest of the slot time (*i.e.*, $\{t^s_{ij} - t(L_P)\}$). The energy dissipation in this case will be multiplied by a factor of $[\rho^s_{ij}(l, L_P) \times \rho^f_{ji}(k, L_A)]/\rho^s_{\text{HS},ij}(l,k)$ considering retransmissions. Hence, the energy dissipation for this case is

$$E^{f,1}_{tx,ij}(l,k) = \left[P_{\text{std}}\{t^s_{ij} - t(L_P)\} + P^{\text{el}}_{tx}(l)t(L_P)\right] \times \frac{\rho^s_{ij}(l, L_P)\rho^f_{ji}(k, L_A)}{\rho^s_{\text{HS},ij}(l,k)}. \tag{9}$$

For the unsuccessful handshake case 3, the transmitter side still consumes $P^{\text{el}}_{tx}(l) \times t(L_P)$ J for data transmission. But the data packet is dropped and the receiver side will not send any ACK

frame back to the intended node. The total energy consumption in this case by considering the retransmission factor of $\rho^f_{ij}(l,L_P)/\rho^s_{\text{HS},ij}(l,k)$ is defined as

$$E^{f,2}_{tx,ij}(l,k) = [P_{\text{std}}\{t^s_{ij} - t(L_P)\} + P^{\text{el}}_{tx}(l)t(L_P)] \times \frac{\rho^f_{ij}(l,L_P)\overbrace{[\rho^s_{ji}(k,L_A) + \rho^f_{ji}(k,L_A)]}^{=1}}{\rho^s_{\text{HS},ij}(l,k)}. \quad (10)$$

In total, the transmitter node spends $E^{tx}_{ij}(l,k) = E^s_{tx,ij}(l,k) + E^{f,1}_{tx,ij}(l,k) + E^{f,2}_{tx,ij}(l,k)$ J of energy.

2) Energy Consumption of the Receiving Node: For the receiver side when we consider the successful handshake (*i.e.*, handshake case 1), $P_{rx} \times t(L_P)$ J of energy is dissipated for data reception, $P^{\text{el}}_{tx}(k) \times t(L_A)$ J for the ACK transmission with power level-k, and $P_{\text{std}} \times \{t^s_{ji} - t(L_P) - t(L_A)\}$ J for standby, respectively. Thus, the total energy expenditure for this case is

$$E^s_{rx,ji}(l,k) = \big[P_{\text{std}}\{t^s_{ji} - t(L_P) - t(L_A)\} + P^{\text{el}}_{tx}(k)t(L_A) + P_{rx}t(L_P)\big] \times \frac{\rho^s_{ij}(l,L_P)\rho^s_{ji}(k,L_A)}{\rho^s_{\text{HS},ij}(l,k)}. \quad (11)$$

For the unsuccessful handshake case 2, the energy cost for the successful data packet reception is $P_{rx} \times t(L_P)$. The ACK packet is transmitted with power level-k, which costs $P^{\text{el}}_{tx}(k) \times t(L_A)$ J of energy. At the rest of the slot time, the receiving node switches to the standby mode, which requires $P_{\text{std}} \times \{t^s_{ij} - t(L_P) - t(L_A)\}$ J of energy. Hence, the total energy consumption including retransmissions can be obtained as

$$E^{f,1}_{rx,ji}(l,k) = \big[P_{\text{std}}\{t^s_{ji} - t(L_P) - t(L_A)\} + P^{el}_{tx}(k)t(L_A) + P_{rx}t(L_P)\big] \times \frac{\rho^s_{ij}(l,L_P)\rho^f_{ji}(k,L_A)}{\rho^s_{\text{HS},ij}(l,k)}. \quad (12)$$

For the unsuccessful handshake case 3, the receiving node cannot receive the transmitted data, hence, in whole slot time, the receiving node is in a standby mode. The total energy dissipation for this case is

$$E^{f,2}_{rx,ji}(l,k) = P_{\text{std}} \times t^s_{ji} \times \frac{\rho^f_{ij}(l,L_P)}{\rho^s_{\text{HS},ij}(l,k)}. \quad (13)$$

In overall, the receiving node consumes $E^{rx}_{ji}(l,k) = E^s_{rx,ji}(l,k) + E^{f,1}_{rx,ji}(l,k) + E^{f,2}_{rx,ji}(l,k)$ J of energy.

C. Optimization Model to Maximize the Network Lifetime

In this part, we present our optimization framework given in Fig. 1 with the objective function of maximizing the network lifetime. Our proposed framework is constructed by using the ILP. The UASN that we consider in this study is denoted as $G(V,E)$, where V is the set of all nodes, while we define set W to stand for the acoustic sensor nodes. The base station is marked as node-1. E is the directed link set. We assume that a sensor node cannot transmit data to itself and the base station

Maximize N_R
Subject to:

$$\sum_{j\in V} f_{ij} - \sum_{j\in W} f_{ji} = N_R \times s_i \ , \forall i \in W \quad (14)$$

$$\sum_{(j,1)\in E} f_{j1} = N_R \sum_{j\in W} s_j \quad (15)$$

$$\sum_{j\in V} E^{tx}_{ij}(l,k) f_{ij} + \sum_{j\in W} E^{rx}_{ji}(l,k) f_{ji} \le \varrho \ , \forall i \in W \quad (16)$$

$$8 \times (L_P + L_A) \times \left(\sum_{j\in V} f_{ij}\lambda^{lk}_{ij} + \sum_{j\in W} \lambda^{lk}_{ji} f_{ji}\right) = \chi_i, \quad \forall i \in V \quad (17)$$

$$\chi_i \le N_R \times T_R \times R \ , \forall i \in V \quad (18)$$

$$f_{ij} \ge 0 \ , \forall (i,j) \in E \quad (19)$$

Fig. 1. ILP model that maximizes network lifetime.

cannot generate data. Our decision variable is denoted with an integer variable f_{ij}, which translates to the number of frames transmitted from node-i to node-j. We organize the network lifetime (*i.e.*, N_R) with rounds and assume that each round lasts 150 s (*i.e.*, $T_R = 150$ s). The network lifetime is defined as the time until the first node depletes its all battery energy [7]. $E^{tx}_{ij}(l,k)$, $E^{rx}_{ji}(l,k)$, and λ^{lk}_{ij} parameters are imported from the preceding subsection.

The constraints of the ILP model are defined in (14)–(19). Constraint (14) is defined for *flow balancing*, which states that for each sensor node (*i.e.*, $\forall i \in W$), incoming traffic (*i.e.*, $\sum_{j\in W} f_{ji}$) plus traffic generated during the lifetime (*i.e.*, $N_R \times s_i$) is equal to the outgoing traffic ($\sum_{j\in V} f_{ij}$). We define Constraint (15) to ensure that all acquired data to be collected at the base station. Constraint (16) is the *energy balancing* constraint that limits the amount of energy consumed for transmission (*i.e.*, $\sum_{j\in V} E^{tx}_{ij}(l,k) f_{ij}$) and reception (*i.e.*, $\sum_{j\in W} E^{rx}_{ji}(l,k) f_{ji}$) to the initial battery energy (*i.e.*, ϱ) at each sensor node. Note that the energy cost for the transmission and reception dominates the total energy dissipation in UASNs [36]. For a Lithium battery with 25 V of voltage and 119-Ah charge capacity, ϱ can be calculated as 10.7 MJ [45]. It is noteworthy to state that the base station does not have such a constraint. We assume that if a node is not in the transmitting, receiving, or standby state, the node can shutdown itself by using a wake up module [35]. Constraint (17) is expressed to calculate the *bandwidth required* (*i.e.*, χ_i—in terms of bits) at each node (including the base station) considering both transmission, reception, and retransmissions. With the help of Constraint (18), we limit the bandwidth utilization to $N_R \times T_R \times R$ (total amount of available bandwidth in terms of bits). Finally, Constraint (19) shows the boundaries of our decision variables.

D. Proposed TPC Approaches

In this subsection, we present the network-level and link-level TPC strategies, which are constructed by using the optimization

model presented in the previous subsection. We aim to quantify the impact of TPC strategies on the OPS and the network lifetime.

1) Network-Level Transmission Power Control (NL-TPC): The network-level TPC approach is straightforward such that a single global transmission power level (*i.e.*, l) is utilized in all links for both data and ACK packet transmissions. We can mathematically model the NL-TPC approach as

$$l_{ij}^{\text{opt}} = k_{ji}^{\text{opt}} = l \quad \forall (i,j) \in E. \tag{20}$$

Note that, in the aforementioned equation, l_{ij}^{opt} denotes the data power level used on link-(i,j), while k_{ji}^{opt} models the ACK transmission power level in the reverse link (*i.e.*, link-(j,i)).

2) Link-Level Transmission Power Control (LL-TPC): We employ the LL-TPC approach as stated in (21) [14]. The idea is to choose best power levels l_{ij}^{opt} and k_{ji}^{opt} for each data and ACK frames on each link-(i,j) such that the total energy dissipation for transmission and reception on link-(i,j) (given as $E_{ij}^{tx}(l,k) + E_{ji}^{rx}(l,k)$) is minimized.

$$\{l_{ij}^{\text{opt}}, k_{ji}^{\text{opt}}\} = \underset{l \in \mathcal{L}, k \in \mathcal{L}}{\text{argmin}} (E_{ij}^{tx}(l,k) + E_{ji}^{rx}(l,k)). \tag{21}$$

IV. Analysis

In this section, we present the results of our investigation on the PSO jointly with the TPC for maximizing the UASN lifetime. We construct our physical model (see Section III-A) and link-layer model (see Section III-B) in MATLAB, while the optimization model (see Section III-C) is built and solved by using GAMS with the CPLEX solver. Throughout the analysis section, we investigate the impact of the NL-TPC and LL-TPC approaches jointly on the network lifetime and optimum frame size in Sections IV-A and IV-B, respectively. We compare the lifetimes for these approaches in Section IV-C. Furthermore, determination of the optimum frame size for several commercial and research underwater modems are presented in Section IV-D. Finally, in Section IV-E, we exactly and heuristically solve the optimization model and provide a comparative analysis on both lifetimes and solution times. Table I shows the parameters used throughout the analysis.

In this study, we construct an optimization framework based on the ILP, and our analyses are performed through the numerical solutions of our model for a wide range of problem instances. Therefore, utilization simulators specifically designed for underwater networks cannot be employed in the solution of the optimization models.

We model our network as a static 3-D UASN [1] where 49 sensor nodes (*i.e.*, $|W| = 49$) are mounted on the bottom of the ocean [46] with the depth of 1 km (*i.e.*, $h = 1000$ m). Since we are working in a deep water channel, effects of multipath are neglected [15]. At the bottom of the ocean, the network deployment area is considered as a disk of radius R_{net} such that sensor nodes are randomly deployed (according to a uniform distribution) within the disk. The base station is mounted under a floating surface station located at the center of the disk, which is anchored to the bottom of the ocean. Hence, the total number of nodes in the network is $|V| = |W| + 1 = 50$. We assume

TABLE I
Simulation Parameters

Channel Parameters		
κ	Spreading factor	2
B_N	Noise bandwidth (kHz)	1
c	Nominal speed of sound in water (m/s)	1500
c_b	Bottom sound speed (m/s)	1800
ρ_s	Seawater density (kg/m^3)	1024
ρ_b	Seabottom density (kg/m^3)	1843
Packet Parameters		
L_A	ACK size (bytes)	20
L_D	Amount of data generated at each round (bytes)	3000
L_H	Header size (bytes)	20
L_{PL}	Payload size (bytes)	3000, 1500, 750, 600, 500, 375, 300, 250, 200, 150, 100, 75, 50, and 30
s_i	Number of data frames generated at each round	1, 2, 3, 4, 5, 6, 8, 10, 12, 15, 20, 30, 40, 50, 60, and 100
Network Parameters		
$\|V\|$	Number of nodes including the base station	50, 100, 200
h	Node depth (m)	500, 1000, 3500
R_{net}	Network radii (km)	14, 16, 18, 20
T_R	Round duration (s)	150
ϱ	Initial battery energy (MJ)	10,7
# of random topologies		200

that coordinates of nodes (including the base station) do not change in time. We choose several R_{net} values (*e.g.*, 14, 16, 18, and 20 km) to examine the impact of the node density on the UASN lifetime. Note that we choose these R_{net} values to work in an extreme underwater environment where the average successful handshake probability values lie within 0.09–0.23. Each data point presented in the subsequent figures is the average of 200 random topologies so that we have the opportunity to analyze the influence of topological changes. Furthermore, for each curve in Figs. 2–5, we present normalized lifetime values, which are obtained by dividing the absolute lifetime values (for each payload size) to the maximum lifetime value (which is obtained with the payload size that yields a maximum lifetime). In the rest of this manuscript, payload sizes are provided in descending order (*i.e.*, 3000, 1500, 750, 600, 500, 375, 300, 250, 200, 150, 100, 75, 50, and 30 bytes) because we are dealing with s_i (*i.e.*, number of data frames produced at each round) given in ascending order (*i.e.*, 1, 2, 3, 4, 5, 6, 8, 10, 12, 15, 20, 30, 40, 50, 60, and 100).

The lifetime maximization problem that we are investigating in this paper has known to have convergecast traffic (*i.e.*, all traffic terminates at the base station) [27]. In addition, with the help of the retransmissions, we assume that all generated data by sensor nodes successfully conveyed to the base station. Nevertheless, the networking mechanism that the ILP model employs at each round is that every sensor nodes generates $L_D = 3000$ bytes of data, which are either fragmented or

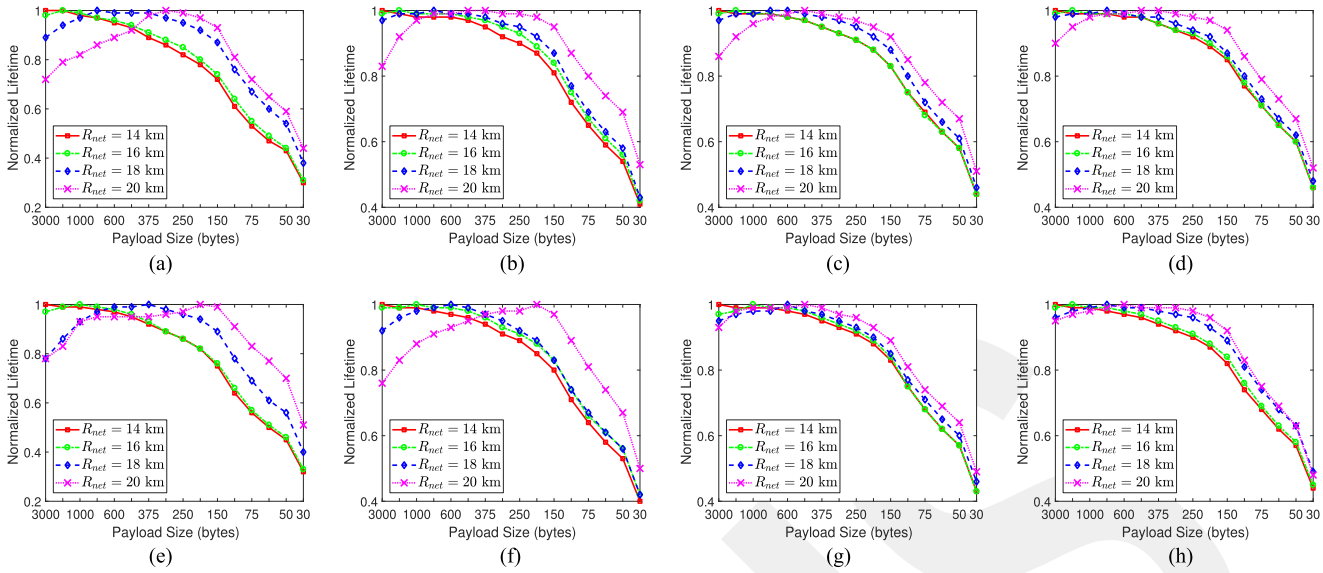

Fig. 2. Normalized lifetimes with respect to payload size (in bytes) and network radii (R_{net}) for the NL-TPC approach employing Urick and BELLHOP models with global transmission power levels are set to 5, 15, 25, and 35 W throughout the network. (a) $P_{tx}^{\text{el}}(l) = 5$ W. Urick. (b) $P_{tx}^{\text{el}}(l) = 15$ W, Urick. (c) $P_{tx}^{\text{el}}(l) = 25$ W, Urick. (d) $P_{tx}^{\text{el}}(l) = 35$ W, Urick. (e) $P_{tx}^{\text{el}}(l) = 5$ W, BELLHOP. (f) $P_{tx}^{\text{el}}(l) = 15$ W, BELLHOP. (g) $P_{tx}^{\text{el}}(l) = 25$ W, BELLHOP. (h) $P_{tx}^{\text{el}}(l) = 35$ W, BELLHOP.

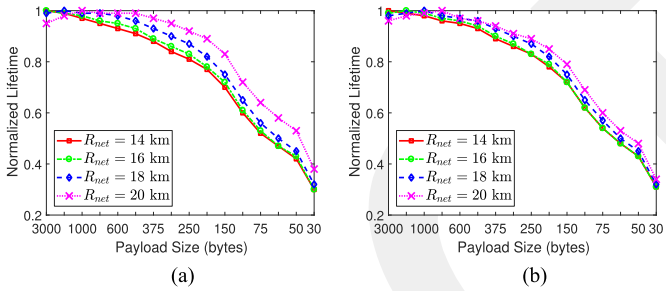

Fig. 3. Normalized lifetimes in terms of seconds with respect to payload size (in bytes) and network radii (R_{net}) for the LL-TPC approach employing Urick and BELLHOP models. (a) Norm. LT, Urick. (b) Norm. LT, BELLHOP.

not; that are successfully conveyed to the base station with the help of retransmissions. Data exchange among nodes requires both transmission and reception energy dissipations, which lessens the remaining battery energy. As the first sensor node depletes its initial battery, the number of rounds that network survives (*i.e.*, N_R) yields the lifetime. The same optimal flow pattern is used for the rest of the rounds in order to maximize the network lifetime. The end-to-end latency for a single sensor node to transmit its own data to the base station is upper bounded by T_R seconds, which is the round duration. In order to see this result, we divide both sides of Constraints (17) and (18) by $N_R \times R$ and obtain the following inequality:

$$\frac{8 \times (L_P + L_A)}{N_R \times R} \times \left(\sum_{j \in V} f_{ij} \lambda_{ij}^{lk} + \sum_{j \in W} \lambda_{ji}^{lk} f_{ji} \right) \leq T_R \quad \forall i \in V. \tag{22}$$

Note that, the right-hand side (RHS) of this modified constraint simply becomes T_R (in seconds) and left-hand side (LHS) of this constraint becomes the amount of time (in seconds) for node-i to transmit and receive data in all directions (including the base station). Our results reveal that the maximum possible network lifetime is around 1 year, which is obtained as $N_R = 207\,360$ rounds when $R_{\text{net}} = 14$ km and $L_{\text{PL}} = 3000$ bytes for the Urick model. For this configuration, we observe that LHS is 7% of the RHS of the inequality 22. Thus, we can state that the average end-to-end latency is upper bounded by 10.5 s.

A. Performance Evaluation of the NL-TPC Approach

In this part of the analysis, we present normalized lifetimes for the NL-TPC approach as a function payload size and R_{net} values in Fig. 2. For each subfigure of this plot, we fix the global transmission power level on all links to 5, 15, 25, and 35 W, respectively. Upper and lower rows of this figure show results for Urick's and BELLHOP channel models, respectively. In this figure, we see that for a dense network (*i.e.*, $R_{\text{net}} = 14$ km), regardless of the channel model used, the OPS is obtained as 3000 bytes. As we increase R_{net}, the successful handshake probability decreases, thus smaller payload sizes yield maximum lifetime values. When considering a highly sparse network (*i.e.*, high R_{net} values), frames with the maximum payload are quite like to be dropped. Since a frame drop incurs a retransmission, more energy would be wasted due to the extra transmission, which leads lesser lifetime values. That is why lower payloads are preferred to prolong the network lifetime for $R_{\text{net}} > 14$ km. Normalized network lifetimes can be reduced to 0.30 [in Fig. 2(a) and (e)] if the smallest payload size (*i.e.*, $L_{\text{PL}} = 30$ bytes) and lowest global transmission power level (*i.e.*, $P_{tx}^{\text{el}}(l) = 5$ W) is used. For a payload size of 30 bytes, each node would generate 100 packets at each round, which

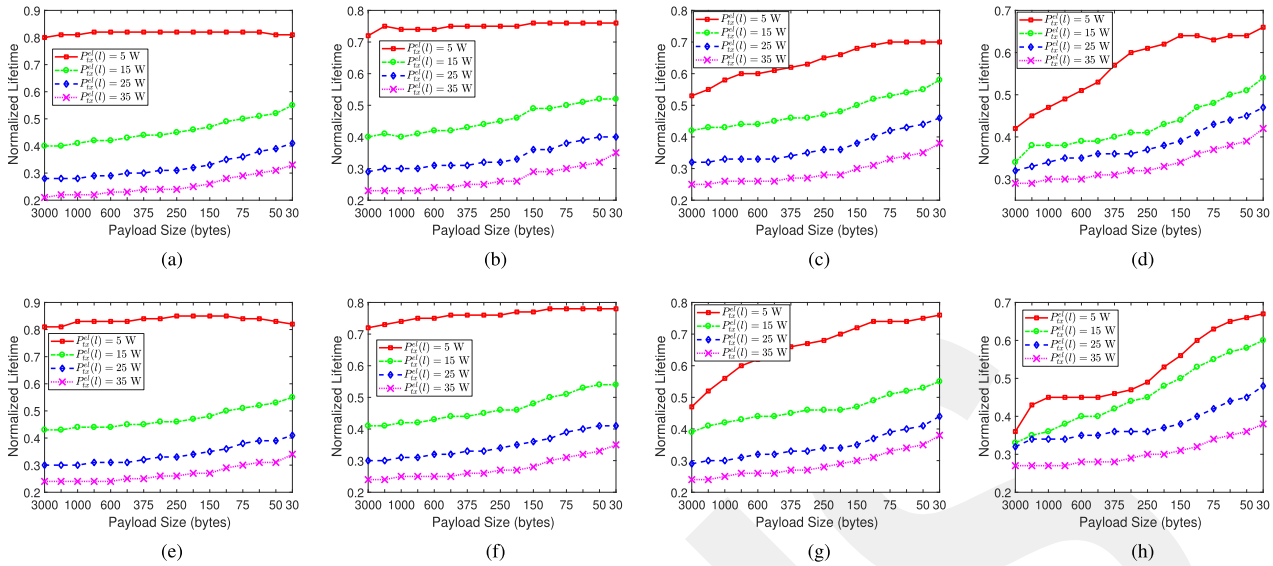

Fig. 4. Normalized network lifetimes for the NL-TPC approach with respect to the LL-TPC approach as a function of network radii (R_{net}—km), global transmission power levels ($P_{tx}^{\text{el}}(l)$ – W), and payload size (bytes) for Urick and BELLHOP models. (a) $R_{\text{net}} = 14$ km, Urick. (b)$R_{\text{net}} = 16$ km, Urick. (c) $R_{\text{net}} = 18$ km, Urick. (d) $R_{\text{net}} = 20$ km, Urick. (f) $R_{\text{net}} = 14$ km, BELLHOP. (g) $R_{\text{net}} = 16$ km, BELLHOP. (h) $R_{\text{net}} = 18$ km, BELLHOP. (i) $R_{\text{net}} = 20$ km, BELLHOP.

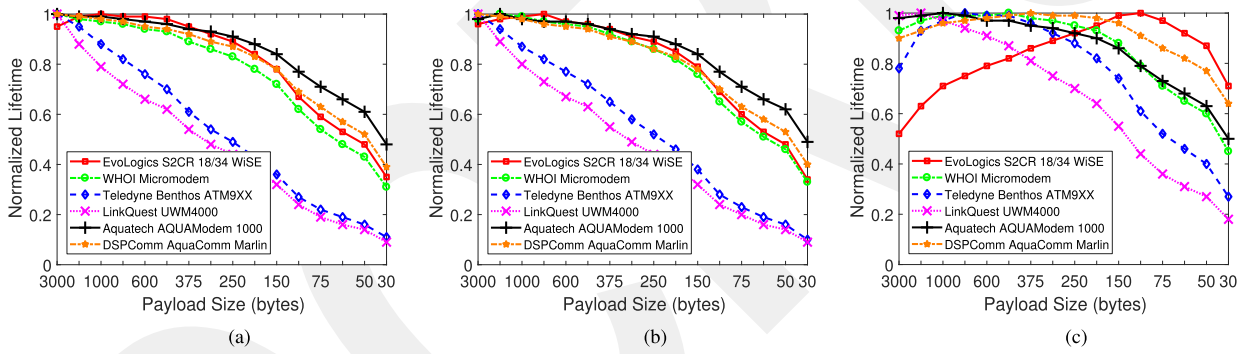

Fig. 5. Normalized network lifetimes for six popular commercial underwater modems and the corresponding optimal packet sizes as a function of depth (h) and payload size (bytes) when network radius is set to 20 km ($R_{\text{net}} = 20$ km) employing the BELLHOP model. (a) Norm. lifetimes when $h = 500$ m. (b) Norm. lifetimes when $h = 1000$ m. (c) Norm. lifetimes when $h = 3500$ m.

results in excessive amount of communication energy dissipation. Hence, the normalized network lifetime rapidly decreases in this case. The OPS values obtained for the BELLHOP model are smaller than the OPS values obtained for Urick's model for sparse networks (*i.e.*, $R_{\text{net}} > 18$ km) when we especially consider low global transmission power levels [in Fig. 2(e) and (f)]. The reason behind this trend is due to the higher transmission loss values (*i.e.*, A_{ij}) of the BELLHOP model. This result becomes visible when the global transmission power levels are low (*i.e.*, $P_{tx}^{\text{el}}(l) = 5$ or 15 W). Furthermore, the increment in the transmission power positively effects the successful frame reception, hence, frames with higher payload sizes yield better normalized lifetimes when compared to the lifetime obtained for the OPS.

B. Performance Evaluation of the LL-TPC Approach

In Fig. 3(a) and (b), we employ the LL-TPC approach and aim to determine the OPS values maximizing network lifetimes for each parameter setting. The most striking result emerged from this analysis is that OPS values are different from the NL-TPC case, which are obtained as 3000, 3000, 1500, and 1000 bytes for Urick's model; 3000, 1500, 1000, and 750 bytes for the BELLHOP model considering $R_{\text{net}} = 14$, 16, 18, and 20 km, respectively. Since transmission loss values for the BELLHOP model are greater than Urick's model, retransmissions occur frequently with the BELLHOP model, which forces lower OPS values to be utilized for lifetime maximization. We also observe that payload sizes smaller than 750 bytes are not preferred because the LL-TPC approach tries to utilize as minimum as possible transmission power levels on each link individually to guarantee a certain successful handshake probability. Our analysis shows that regardless of the channel model used, average transmission powers (i.e., $[\sum_{(i,j)\in E} l_{ij}^{\text{opt}} \times f_{ij}]/\sum_{(i,j)\in E} f_{ij}$) are calculated in the interval 6.00–8.62 W for the LL-TPC approach. Similar to the NL-TPC approach, normalized network lifetimes can be reduced to 0.30 if the smallest payload size (*i.e.*, $L_{\text{PL}} = 30$ bytes) is used.

TABLE II

MAX. TRANSMIT POWER LEVEL-l (MAX$[P_{tx}^{\text{EL}}(l)]$ IN WATT), RECEPTION POWER (P_{rx} IN WATT), STANDBY/IDLE POWER (P_{std} IN MILLIWATT), CENTRAL OPERATING FREQUENCY (f IN KILOHERTZ), AND DATA RATE (R IN KILOBIT PER SECOND) OF SIX COMMERCIAL AND RESEARCH UNDERWATER MODEMS [22]

Underwater Modem	max$[P_{tx}^{el}(l)]$ (W)	P_{rx} (W)	P_{std} (mW)	f (kHz)	R (kbps)
EvoLogics S2CR 18/34 WiSE	35	1.3	2.5	26	13.90
WHOI Micromodem	48	3	8	25	5
Teledyne Benthos ATM9XX	20	0.77	16.8	24.50	15.36
LinkQuest UWM4000	7	0.8	8	17	8.50
Aquatech AQUAModem 1000	20	0.6	1	9.75	2
DSPComm AquaComm Marlin	1.8	0.25	1.8	23	0.48

C. Comparison of NL-TPC and LL-TPC Approaches

In Fig. 4, we present a detailed comparison of normalized network lifetimes for the NL-TPC and LL-TPC approaches as a function of R_{net} and payload sizes for both channel models. In this figure, the NL-TPC lifetimes are normalized with the LL-TPC lifetimes (LL-TPC lifetimes are taken as 1.00). Regardless of the network size, normalized NL-TPC lifetimes are between 0.42 and 0.82 and 0.36 and 0.85 when $P_{tx}^{\text{el}}(l) = 5$ W for Urick and BELLHOP models, respectively. As the transmission power increases to 35 W, normalized lifetimes for the NL-TPC are in the intervals 0.21–0.42 and 0.23–0.38 for Urick and BELLHOP models, respectively. Utilization of high power levels causes network to dissipate the excessive amount of energy, hence, normalized lifetimes are decreased. As a general trend, normalized lifetimes decrease as the payload size increases due to the wastage of energy for frequent retransmissions when the payload size increases. This result is much visible for highly sparse networks (*e.g.*, $R_{\text{net}} > 16$ km).

D. OPS Values of Several Underwater Modems

In this part of the analysis, we determine the OPS values for six popular commercial and research underwater modems. Besides the EvoLogics S2CR 18/34 WiSE modem, we choose WHOI Micromodem, Teledyne Benthos ATM9XX, LinkQuest UWM4000, Aquatech AQUAModem 1000, and DSPComm AquaComm Marlin modems, which are the most famous underwater modems available in the market and academia. $P_{tx}^{\text{el}}(l)$, f, R, P_{rx}, and P_{std} values of these modems are adopted from [22] and reported in Table II. We also quantify the impact of depth on the determination of OPS values for these modems. For this purpose, we choose the BELLHOP model as the channel model, employ the LL-TPC approach (each modem is assumed to have five discrete power levels), fix the network radius to 20 km, and choose depth values as 500, 1000, and 3500 m. We present the normalized lifetimes with corresponding OPS values in Fig. 5 for this parameter configuration. Except for the EvoLogics S2CR 18/34 WiSE modem, OPS values are obtained as 3000 bytes regardless of the modem platform when $h = 500$ m. For this depth, OPS of EvoLogics S2CR 18/34 WiSE modem is observed as 750 bytes. OPS values start to differ as the depth of the network increases. Our results reveal that OPS values can be as high as 1500 bytes (in Fig. 5(c)—LinkQuest UWM4000 modem) and as low as 100 bytes (in Fig. 5(c)—EvoLogics S2CR 18/34 WiSE modem) when $h = 3500$ m.

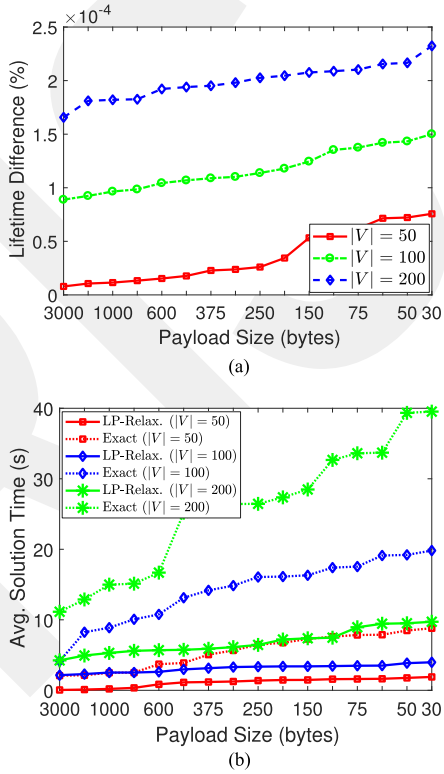

Fig. 6. (a) Avg. lifetime differences in the percentage between the exact ILP and LP-relaxation solutions and (b) avg. solution times in seconds as a function of payload size and number of nodes in the network employing the BELLHOP model for the LL-TPC approach when $R_{\text{net}} = 20$ km and $h = 1000$ m. (a) Avg. lifetime differences (%). (b) Avg. solution times (s).

E. Time Complexity Analysis of the ILP Model

The optimization model that maximizes the network lifetime is an ILP problem, which is known to be an NP-complete problem. Since the computation time for NP-complete problems are high, the number of nodes in the network negatively effects the computation time due to the increment of the search space of the f_{ij} integer variable. It is critical to develop some heuristic methods to solve these problems in polynomial time. One of these heuristic methods is known to be linear programming (LP) relaxation where the integer variables of the ILP model are taken as continuous variables. LP-relaxation converts the ILP model to LP model and since the LP problems are solved in polynomial time.

We present the lifetime differences (in percentage) and solution times between both with exact integer and LP-relaxation methods in Fig. 6(a) as a function of payload size and number of EvoLogics S2C 18/34 WiSE nodes in the network (*i.e.*, $|V| =$ 50, 100, and 200 nodes) employing the BELLHOP model for the LL-TPC approach when $R_{\text{net}} = 20$ km and $h = 1000$ m. We observe that lifetime difference increases as the payload size decreases, however, this increment can be neglected since the lifetime difference is in the order of 10^{-5}. Furthermore, as the number of nodes in the network increases, the lifetime difference also increases due to the extra f_{ij} variables included in the ILP model. Nonetheless, we observe that the maximum lifetime difference between the exact and LP-relaxation solution is obtained as 0.00023% (when $|V| = 200$ for $L_{\text{PL}} = 30$ bytes). We also observe from Fig. 6(b) that LP-relaxation solutions take significantly lower computation times when compared to exact ILP solutions. Finally, as the number of nodes in the network increases, the solution times for both exact ILP and LP-relaxation increases but we can say that the maximum solution time for the LP-relaxation approach does not exceed 10 s. Finally, our analysis reveals that choice of different modem platforms has insignificant effects on the results.

V. Conclusion

In this paper, a realistic link-layer energy consumption abstraction for UASNs is proposed by using the power consumption characteristics of the EvoLogics S2C 18/34 WiSE underwater acoustic node platform, which sits on the top of two different acoustic propagation models (*i.e.*, an empirical approximate model and accurate underwater propagation tool which can perform ray tracing). We also propose an optimization framework via the ILP to jointly optimizes the transmission power and frame size to maximize the network lifetime. We construct two TPC approaches by using the proposed optimization model. We perform our analysis in a wide range of parameter space (*e.g.*, node density, transmission power, *etc.*). We further determine optimal frame sizes for several underwater modems and provide a time complexity analysis of the optimization framework. Our main conclusions are itemized as follows.

1) There exists an optimal frame size where the network lifetime can be maximized, which depends on the channel conditions, network density, underwater modem platform, and TPC approach that is employed.
2) For successful handshake probabilities greater than 0.23, the optimum frame size would be as highest as possible to reduce the extra transmission energy costs due to the retransmissions and fragmentation. As the underwater channel conditions become much worse, smaller frames that are prone to frame drops yield a maximized network lifetime.
3) Although the NL-TPC scheme is easy to be implemented in UASNs, such an approach may underestimate the network lifetime at least 18% when compared to the LL-TPC approach due to the wastage of energy dissipation.
4) Determination of optimal packet sizes should be decided jointly with the transmission power control approaches in order to maximize the network. The optimum frame size that yields a maximized lifetime for the NL-TPC approach may not be suitable for the LL-TPC approach.
5) Joint optimization of the packet size and transmission power has never been incorporated into any practical underwater acoustic communication applications, possibly, due to the lack of the analysis to determine the effects of such optimization on system performance. However, our results that address the gap in the literature, clearly, reveal that joint optimization of the packet size and transmission power has a significant impact on the network lifetime optimization in UASNs. Therefore, future practical UASN architects must incorporate joint optimization of the packet size and transmission power in their designs.

Future work includes extending the proposed optimization framework by jointly optimizing the operating frequency, TPC approach, and packet size for various UASN applications.

References

[1] I. F. Akyildiz, D. Pompili, and T. Melodia, "Underwater acoustic sensor networks: Research challenges," *Ad Hoc Netw.*, vol. 3, no. 3, pp. 257–279, 2005.
[2] J. Jiang, G. Han, L. Shu, S. Chan, and K. Wang, "A trust model based on cloud theory in underwater acoustic sensor networks," *IEEE Trans. Ind. Inform.*, vol. 13, no. 1, pp. 342–350, Feb. 2017.
[3] S. Basagni, C. Petrioli, R. Petroccia, and M. Stojanovic, "Optimized packet size selection in underwater wireless sensor network communications," *IEEE J. Ocean. Eng.*, vol. 37, no. 3, pp. 321–337, Jul. 2012.
[4] T. M. Chiwewe and G. P. Hancke, "A distributed topology control technique for low interference and energy efficiency in wireless sensor networks," *IEEE Trans. Ind. Informat.*, vol. 8, no. 1, pp. 11–19, Feb. 2012.
[5] X. Jin, Y. Chen, and X. Xu, "The analysis of hops for multi-hop cooperation in underwater acoustic sensor networks," in *Proc. IEEE/OES China Ocean Acoust.*, 2016, pp. 1–5.
[6] Z. Zhou, W. Fang, J. Niu, L. Shu, and M. Mukherjee, "Energy-efficient event determination in underwater WSNs leveraging practical data prediction," *IEEE Trans. Ind. Informat.*, vol. 13, no. 3, pp. 1238–1248, Jun. 2017.
[7] G. Tuna and V. C. Gungor, "A survey on deployment techniques, localization algorithms, and research challenges for underwater acoustic sensor networks," *Int. J. Commun. Syst.*, vol. 30, no. 17, 2017, Art. no. p. e3350.
[8] M. Stojanovic, "Optimization of a data link protocol for an underwater acoustic channel," in *Proc. Europe Oceans*, vol. 1, 2005, pp. 68–73.
[9] M. Ayaz, L. T. Jung, A. Abdullah, and I. Ahmad, "Reliable data deliveries using packet optimization in multi-hop underwater sensor networks," *Jo. King Saud University, Computer Inform. Sci.*, vol. 24, no. 1, pp. 41–48, 2012.
[10] M. C. Vuran and I. F. Akyildiz, "Cross-layer packet size optimization for wireless terrestrial, underwater, and underground sensor networks," in *Proc. IEEE Conf. Comput. Commun.*, 2008, pp. 780–788.
[11] W. Ahmad, K. M. Awan, and K. Iqbal, "Dynamic length packet size communication technique for underwater sensor networks," in *Proc. Int. Conf. Intell. Syst. Eng.*, 2016, pp. 242–249.
[12] M. Molins and M. Stojanovic, "Slotted FAMA: A MAC protocol for underwater acoustic networks," in *Proc. OCEANS Asia Pacific*, 2006, pp. 1–7.
[13] X. Guo, M. R. Frater, and M. J. Ryan, "A propagation-delay-tolerant collision avoidance protocol for underwater acoustic sensor networks," in *Proc. OCEANS, Asia Pacific*, 2006, pp. 1–6.
[14] H. U. Yildiz, B. Tavli, and H. Yanikomeroglu, "Transmission power control for link-level handshaking in wireless sensor networks," *IEEE Sensors J.*, vol. 16, no. 2, pp. 561–576, Jan. 2016.
[15] D. Pompili, T. Melodia, and I. F. Akyildiz, "A CDMA-based medium access control for underwater acoustic sensor networks," *IEEE Trans. Wireless Commun.*, vol. 8, no. 4, pp. 1899–1909, Apr. 2009.
[16] A. Castagnetti, A. Pegatoquet, T. N. Le, and M. Auguin, "A joint duty-cycle and transmission power management for energy harvesting WSN," *IEEE Trans. Ind. Informat.*, vol. 10, no. 2, pp. 928–936, May 2014.

[17] E. M. Sozer, M. Stojanovic, and J. G. Proakis, "Underwater acoustic networks," *IEEE J. Ocean. Eng.*, vol. 25, no. 1, pp. 72–83, Jan. 2000.
[18] P. Xie and J. H. Cui, "Exploring random access and handshaking techniques in large-scale underwater wireless acoustic sensor networks," in *Proc. OCEANS*, 2006, pp. 1–6.
[19] H. H. Ng, W. S. Soh, and M. Motani, "MACA-U: A media access protocol for underwater acoustic networks," in *Proc. IEEE Global Telecommun. Conf.*, 2008, pp. 1–5.
[20] M. B. Porter and H. P. Bucker, "Gaussian beam tracing for computing ocean acoustic fields," *J. Acoustical Soc. Amer.*, vol. 82, no. 4, pp. 1349–1359, 1987.
[21] M. Stojanovic, "On the relationship between capacity and distance in an underwater acoustic communication channel," in *Proc. ACM Int. Workshop Underwater Netw.*, 2006, pp. 41–47.
[22] S. Sendra, J. Lloret, J. M. Jimenez, and L. Parra, "Underwater acoustic modems," *IEEE Sensors J.*, vol. 16, no. 11, pp. 4063–4071, Jan. 2016.
[23] A. Akbas, H. U. Yildiz, and B. Tavli, "Data packet length optimization for wireless sensor network lifetime maximization," in *Proc. Int. Conf. Commun.*, 2014, pp. 1–6.
[24] A. Akbas, H. U. Yildiz, B. Tavli, and S. Uludag, "Joint optimization of transmission power level and packet size for WSN lifetime maximization," *IEEE Sensors J.*, vol. 16, no. 12, pp. 5084–5094, Jun. 2016.
[25] M. C. Oto and O. B. Akan, "Energy-efficient packet size optimization for cognitive radio sensor networks," *IEEE Trans. Wireless Commun.*, vol. 11, no. 4, pp. 1544–1553, Apr. 2012.
[26] K. S. Deepak and A. V. Babu, "Packet size optimization for energy efficient cooperative wireless body area networks," in *Proc. IEEE India Conf.*, 2012, pp. 736–741.
[27] S. Kurt, H. U. Yildiz, M. Yigit, B. Tavli, and V. C. Gungor, "Packet size optimization in wireless sensor networks for smart grid applications," *IEEE Trans. Ind. Electron.*, vol. 64, no. 3, pp. 2392–2401, Mar. 2017.
[28] D. Pompili, T. Melodia, and I. F. Akyildiz, "Routing algorithms for delay-insensitive and delay-sensitive applications in underwater sensor networks," in *Proc. Int. Conf. Mobile Comput. Netw.*, 2006, pp. 298–309.
[29] S. Basagni, C. Petrioli, R. Petroccia, and M. Stojanovic, "Choosing the packet size in multi-hop underwater networks," in *Proc. IEEE OCEANS Sydney*, 2010, pp. 1–9.
[30] S. Basagni, C. Petrioli, R. Petroccia, and M. Stojanovic, "Optimizing network performance through packet fragmentation in multi-hop underwater communications," in *Proc. IEEE OCEANS Sydney*, 2010, pp. 1–7.
[31] L. T. Jung and A. B. Abdullah, "Underwater wireless network energy efficiency and optimal data packet size," in *Proc. Int. Conf. Elect., Control Comput. Eng.*, 2011, pp. 178–182.
[32] T. Nguyen, T. M. Hoang, and T. N. Lang, "A study on link quality in single hop sensor networks with brownian motion," in *Proc. Int. Conf. Recent Advances Signal Process., Telecommun. Comput.*, 2017, pp. 235–239.
[33] K. S. Geethu and A. V. Babu, "Energy optimal channel attempt rate and packet size for ALOHA based underwater acoustic sensor networks," *Telecommun. Syst.*, vol. 65, no. 3, pp. 429–442, 2017.
[34] V. Rodoplu and M. K. Park, "An energy-efficient MAC protocol for underwater wireless acoustic networks," in *Proc. MTS/IEEE OCEANS*, vol. 2, 2005, pp. 1198–1203.
[35] EvoLogics, "Underwater acoustic modem S2CR 18/34 white line science edition (WiSE) product information," 2017. [Online]. Available: https://www.evologics.de/files/DataSheets/EvoLogics_S2CR_1834_WiSE_Product_Information.pdf
[36] R. Su, R. Venkatesan, and C. Li, "Balancing between robustness and energy consumption in underwater acoustic sensor networks," in *Proc. IEEE Wireless Commun. Netw. Conf.*, 2015, pp. 1048–1053.
[37] M. Zorzi, P. Casari, N. Baldo, and A. F. Harris, "Energy-efficient routing schemes for underwater acoustic networks," *IEEE J. Sel. Areas Commun.*, vol. 26, no. 9, pp. 1754–1766, Dec. 2008.
[38] S. Gul, S. S. H. Zaidi, R. Khan, and A. B. Wala, "Underwater acoustic channel modeling using BELLHOP ray tracing method," in *Proc. Int. Bhurban Conf. Appl. Sci. Technol.*, 2017, pp. 665–670.
[39] C. Petrioli, R. Petroccia, J. R. Potter, and D. Spaccini, "The SUNSET framework for simulation, emulation and at-sea testing of underwater wireless sensor networks," *Ad Hoc Netw.*, vol. 34, pp. 224–238, 2015.
[40] R. Masiero *et al.*, "DESERT underwater: An NS-Miracle-based framework to design, simulate, emulate and realize test-beds for underwater network protocols," in *Proc. IEEE Oceans Yeosu*, 2012, pp. 1–10.
[41] S. R. Thompson, "Sound propagation considerations for a deep-ocean acoustic network," Ph.D. dissertation, Naval Postgraduate School, Monterey, CA, USA, 2009.
[42] J. Llor and M. P. Malumbres, "Statistical modeling of large-scale signal path loss in underwater acoustic networks," *Sensors*, vol. 13, no. 2, pp. 2279–2294, 2013.
[43] E. M. Rubino *et al.*, "Progressive image compression and transmission with region of interest in underwater robotics," in *Proc. OCEANS Aberdeen*, 2017, pp. 1–9.
[44] L. Hong, F. Hong, Z. W. Guo, and X. Yang, "A TDMA-based MAC protocol in underwater sensor networks," in *Proc. Int. Conf. Wireless Commun., Netw. Mobile Comput.*, 2008, pp. 1–4.
[45] EvoLogics, "S2C battery packs,"2017. [Online]. Available: https://www.evologics.de/en/products/Accessories/s2cr_battery_packs.html
[46] A. Stefanov and M. Stojanovic, "Design and performance analysis of underwater acoustic networks," *IEEE J. Sel. Areas Commun.*, vol. 29, no. 10, pp. 2012–2021, Dec. 2011.

Huseyin Ugur Yildiz (S'13–M'16) received the B.S. degree in electrical and electronics engineering from Bilkent University, Ankara, Turkey, in 2009, and the M.S. and Ph.D. degrees in electrical and electronics engineering from the TOBB University of Economics and Technology, Ankara, in 2013 and 2016, respectively.

He is an Assistant Professor with the Department of Electrical and Electronics Engineering, TED University, Ankara, Turkey. His research interests include the applications of optimization techniques for modeling and analyzing research problems on wireless communications, wireless networks, underwater acoustic networks, and smart grids.

Vehbi Cagri Gungor received the B.S. and M.S. degrees in electrical and electronics engineering from Middle East Technical University, Ankara, Turkey, in 2001 and 2003, respectively, and the Ph.D. degree in electrical and computer engineering from the Broadband and Wireless Networking Laboratory, Georgia Institute of Technology, Atlanta, GA, USA, in 2007.

He is currently an Associate Professor and the Chair with Computer Engineering Department, Abdullah Gul University, Kayseri, Turkey. His current research interests include next-generation wireless networks, wireless ad hoc and sensor networks, smart grid communications, and underwater networks.

Bulent Tavli (S'97–M'05–SM'17) received the B.S. degree in electrical and electronics engineering from Middle East Technical University, Ankara, Turkey, in 1996, and the M.S. and Ph.D. degrees in electrical and computer engineering from the University of Rochester, Rochester, NY, USA, in 2002 and 2005, respectively.

He is a Professor with the Department of Electrical and Electronics Engineering, TOBB University of Economics and Technology, Ankara. His current research interests include wireless communications, networking, optimization, embedded systems, information security, and smart grids.